Applied Catalysis B: Environmental 100 (2010) 310–317

Contents lists available at ScienceDirect

Applied Catalysis B: Environmental

journal homepage: www.elsevier.com/locate/apcatb

Wet air oxidation of trinitrophenol with activated carbon catalysts: Effect of textural properties on the mechanism of degradation

Sergio Morales-Torres[a], Adrián M.T. Silva[b,*], Agustín F. Pérez-Cadenas[a], Joaquim L. Faria[b], Francisco J. Maldonado-Hódar[a], José L. Figueiredo[b], Francisco Carrasco-Marín[a]

[a] Departamento de Química Inorgánica, Facultad de Ciencias, Universidad de Granada, Campus Fuentenueva s/n, 18071 Granada, Spain
[b] Laboratório de Catálise e Materiais (LCM), Laboratório Associado LSRE/LCM, Departamento de Engenharia Química, Faculdade de Engenharia, Universidade do Porto, Rua Dr. Roberto Frias s/n, 4200-465 Porto, Portugal

ARTICLE INFO

Article history:
Received 27 May 2010
Received in revised form 30 July 2010
Accepted 5 August 2010
Available online 12 August 2010

Keywords:
Catalytic wet air oxidation
Trinitrophenol
Activated carbon
Textural properties

ABSTRACT

Activated carbons (ACs), with different activation degrees, were obtained by chemical activation of olive stones and tested for the removal of 2,4,6-trinitrophenol (TNP) from aqueous solutions by catalytic wet air oxidation (CWAO). These materials were characterized using different techniques (e.g., N_2 and CO_2 adsorption, temperature programmed desorption, immersion calorimetry and scanning electron microscopy). The non-catalytic oxidation of TNP in water, at 473 K and 0.7 MPa of oxygen partial pressure, is negligible, while the use of ACs as catalysts leads to complete removal of this organic compound. Competition between adsorption and catalytic oxidation reaction pathways, occurring simultaneously in the CWAO process, depends on the carbon porous texture. The extent of oxidation is given by the amount of nitrates formed during reaction. When a highly microporous carbon with large surface area (S_{BET} = 1530 m^2/g) is used, all dissolved TNP is adsorbed and oxidation takes place in wide micropores. However, when using a carbon material with low surface area (S_{BET} = 121 m^2/g) and low microporosity, TNP degradation will also occur on the external surface area, since there is enough TNP available in the bulk liquid media; in this case fast degradation takes place on the carbon macro–mesopores. Following that, the degradation mechanism is always heterogeneous but takes place in different ranges of porosity and depends on the amount of dissolved TNP. In addition, the surface chemistry of the carbon materials is modified during the CWAO process due to the presence of oxygen at the conditions employed.

1. Introduction

The use of biomass residues to prepare ACs suitable for water treatment is an important task, because the abundance and the universal distribution of this kind of residues allows the preparation of very valuable products that can improve the quality of water in many developing countries. Thus, pruning rests, wood, almond shell, coconut, and in this case, olive stones, can be transformed in carbon materials with different textural properties depending on the activation degree and procedure [1–5]. Because the raw materials are cheap, the carbon materials prepared also result to be cheap, which favour their applications in water treatments.

In this work, 2,4,6-trinitrophenol (TNP) was selected as target molecule for testing the efficiency of the treatment method. TNP is an explosive, a colouring agent and an agrochemical, also known as picric acid, with worldwide permissible thresholds of up to 20 ppb in water [6]. TNP is also a by-product of the industrial synthesis of nitrobenzene. The resulting waste is an aqueous stream at the processing temperature (above 348 K) and a solid when left at ambient temperature. Wet air oxidation (WAO) is a liquid phase process for the treatment of organic pollutants operating at high reaction temperatures (473–593 K) and pressures (2–20 MPa) and using air to generate active oxygen species such as hydroxyl ($HO^{\bullet}$) and hydroperoxyl ($HOO^{\bullet}$) radicals [7]. In CWAO the organic pollutants are oxidized at less severe temperatures (400–523 K) and pressures (0.5–5.0 MPa) in the presence of a catalyst. The use of active catalysts can reduce the reaction temperature, in such a way that the raw effluent resulting from the nitrobenzene synthesis can be treated *in situ*, taking advantage of the high temperature at which it is released, and therefore, allowing for important energy savings. Ideally, the total mineralization of pollutants into CO_2, N_2 and H_2O is preferred. Nevertheless, an increase of the effluent biodegradability by producing easily biodegradable by-products, such as low molecular weight carboxylic acids, can also be appropriate [8]. The final yield will depend on the reaction conditions and catalyst activity.

Several metal oxides (e.g., Cu, Zn, Mn, Fe, Co, and Bi) and noble metals (e.g., Ru, Pt, Pd and Rh) supported on CeO_2, Al_2O_3, ZrO_2,

* Corresponding author. Tel.: +351 225081998; fax: +351 225081449.
E-mail address: adrian@fe.up.pt (A.M.T. Silva).

0926-3373/$ – see front matter © 2010 Elsevier B.V. All rights reserved.
doi:10.1016/j.apcatb.2010.08.007

Table 1
Experimental conditions used to prepare the C500, C600 and C800 carbon materials, and respective percentage of volatiles.

Carbon	Activation T (K)	Ratio of olive stones:KOH	Yield (%)	Ash content (%)
C500	773	1:2	14.7	2.7
C600	873	1:2	13.8	2.2
C800	1073	1:1	13.7	2.8

TiO_2 or carbon materials have been used as heterogeneous catalysts in CWAO in the last four decades [9–15]. The usual deactivation phenomenon observed with metal oxides is the dissolution of the active metals to the liquid phase (leaching) [2]. For this reason, carbon materials are preferred in many cases for CWAO, since they can be used directly in the process as catalysts [1–5,16–21], without the production of contamination by metal lixiviation, and with a very good stability, taking into account that carbon materials are stable in both acidic and alkaline media.

Commercial ACs [1–4,17–20], carbon xerogels [16,18], multi-walled carbon nanotubes (MWCNTs) [22,23], carbon foams and fibres enriched with nitrogen [5] were already tested in the metal-free oxidation of different organic pollutants (e.g., phenol, aniline, chlorophenols and nitrophenols) and aqueous ammonia [1]. Non-catalytic WAO is known to be a homogeneous radical initiated reaction, but the nature of the catalytic process is still a matter of discussion [17]. The reaction can be considered to be purely heterogeneous or a homogeneous oxidation induced by oxygenated radicals generated at the carbon surface [22,23]. In addition, fundamental investigation to understand the effect of the physical and chemical properties of the carbon materials on their performance has gained attention, because the texture and surface chemistry of carbons can affect the adsorption and catalytic properties of these materials [1,18,24]. In the present work, ACs obtained from olive stones with varying textures were used as catalysts in the CWAO of TNP in order to understand the role of these ACs in this process applied for the treatment of wastewaters.

2. Experimental

2.1. Catalysts preparation

ACs were prepared from olive stones by chemical activation using KOH following a method similar to that reported elsewhere [25]. Three different activation temperatures were used, 773, 873 and 1073 K, and these ACs are hereafter referred as C500, C600 and C800, respectively (reference based on the activation temperature in °C). The KOH/stones ratio was 2/1 for C500 and C600, while a ratio of 1/1 was used in the case of C800. Samples were ground and sieved to obtain a particle size below 100 μm. The ash content of all the prepared ACs was around 2.5%, determined by burning a fraction of sample up to 1073 K in air. The experimental conditions used in the synthesis as well as the respective ash contents are gathered in Table 1. As can be observed, the yield and, consequently, the ash contents, were similar for all the prepared ACs.

2.2. Catalyst characterization

The textural characterization of materials was based on the N_2 and CO_2 adsorption isotherms determined at 77 and 273 K, respectively, with a Quantachrome Autosorb-1 apparatus. Previous degassing of samples was performed for 12 h at 373 K. The BET [26] equation was used to estimate the apparent surface area (S_{BET}). The mean micropore width (L_0) and the surface area of the micropores (S_{CO_2}) were obtained from the CO_2 adsorption data by the Stoeckli equations and the micropore volume (W_0) was obtained by applying the Dubinin–Radushkevich equation [27,28]. Mercury porosimetry was performed up to a pressure of 345 MPa in a Quantachrome Autoscan 60 equipment, measuring the external surface area (S_{ext}), the macropore volume (V_{macro}) corresponding to pores with diameters higher than 50 nm, while the mesopore volume (V_{meso}) determined by this technique corresponds to pores with diameters between 3.7 and 50 nm (the mesopore volume range is defined as 2–50 nm [29]).

The morphology of ACs was assessed by scanning electron microscopy (SEM) using a LEO (Carl Zeiss) GEMINI-1530 microscope. The surface chemistry of the prepared carbons was characterized by temperature programmed desorption (TPD) as described elsewhere [30–33] and by the pH_{PZC} (point zero of charge). The pH_{PZC} was determined according the previously published methodology [34], and corresponds to the pH of 250 mg carbon dispersed in 4 mL H_2O at equilibrium and 298 K. TPD spectra were recorded with an automated AMI-200 apparatus for catalyst characterization (Altamira Instruments) equipped with a quadrupole mass spectrometer (Ametek, Mod. Dymaxion). The catalyst sample (0.10 g) was placed in a U-shaped quartz tube inside an electrical furnace and heated under a constant helium flow of 25 cm^3 min^{-1} (STP), at 5 K min^{-1} up to 1373 K. Selected mass signals, m/z = 28 and 44, were monitored during the thermal analysis. The amounts of CO and CO_2 were calibrated at the end of each analysis with CO and CO_2 gases. Since one of the fragments in the mass spectrum of CO_2 occurs at m/z = 28, the mass signal monitored for quantification of CO (m/z = 28) was corrected in order to eliminate the influence of CO_2 on CO evolution [32,33].

The ACs were also analyzed by immersion calorimetry. The immersion enthalpies of the outgassed samples (383 K for 12 h) into aqueous solution of TNP (125 mg L^{-1}) were measured at 303 K with an isothermal calorimeter of the Tian-Calvet type, Setaram C-80-D as described in [35]. Corrections corresponding to the bulb breaking energy and to the liquid vapourization energy were performed.

2.3. Reaction and analysis procedure

The TNP oxidation experiments were carried out in a 160 mL 316-stainless steel high pressure batch reactor (Parr Instruments). In a typical run, 75 mL of a TNP solution (125 mg L^{-1}) were placed into the reactor. The reactor was flushed with pure nitrogen in order to remove dissolved oxygen, pressurized with 0.5 MPa of nitrogen and pre-heated up to the desired temperature (473 K) in 60 min. After this period of time, referred hereafter as t = 0 min, pure air was introduced in order to obtain a final total pressure of 5.5 MPa (corresponding to an oxygen partial pressure of 0.7 MPa). Stirring was maintained at 500 rpm in order to ensure proper mass transfer of air in the liquid phase [16,18]. In the catalytic experiments, 0.2 g L^{-1} of carbon material was used as catalyst. A non-catalytic blank experiment was performed in the absence of catalyst (WAO). In order to discriminate between the adsorption and catalytic components of the TNP removal, adsorption experiments were performed under identical experimental conditions (P, T, amount of catalyst), but replacing air by pure nitrogen. The vapour–liquid equilibrium at these conditions was quantified by using the TNP solution without carbon material in a pure nitrogen atmosphere. Samples were periodically withdrawn and analyzed by high performance liquid chromatography (HPLC), and the catalyst was recovered at the end of the catalytic runs for further characterization.

2.4. Analytical techniques

The concentrations of TNP and nitrates in liquid samples were monitored by HPLC with a Hitachi Elite LaChrom system equipped with a Diode Array Detector (L-2450). An isocratic method of an A:B (40:60) mixture of 3% acetic acid and 1% acetonitrile in methanol

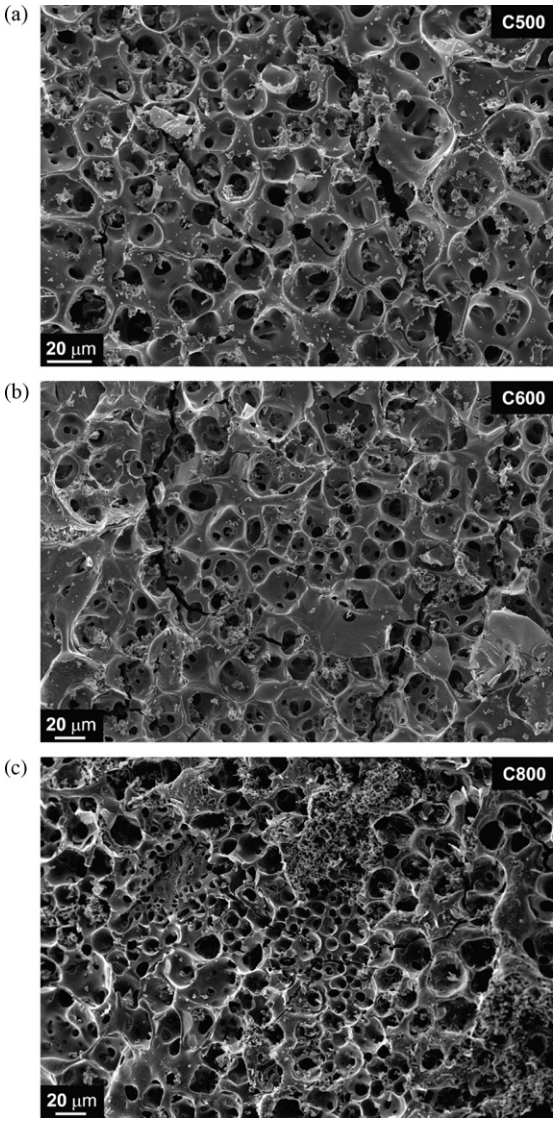

Fig. 1. SEM micrographs of the original ACs (a) C500, (b) C600 and (c) C800.

(A) and 3% acetic acid in water (B) was used with a Purospher Star RP-18 column (250 mm × 4.6 mm; 5 μm particles) for TNP determination. Nitrates were analyzed in another column, Hydrosphere C18 (250 mm × 4.6 mm; 5 μm particles), with an A:B (95:5) mixture of 20 mM NaH_2PO_4 acidified with H_3PO_4 at pH 2.80 (A) and acetonitrile (B). The flow rate in both methods was maintained at 1 mL min^{-1}, and the quantification of TNP and nitrates was based on their respective maximum absorbance in the chromatograms, taken using the EZChrom Elite chromatography data handling software (Version 3.1.7). Absorbance was found to be linear over the whole range considered (maximum relative standard deviation of 2%). The dissolved organic carbon (DOC) was also determined for selected samples using a Shimadzu TOC-5000A analyzer. The uncertainty in this parameter, defined as the relative deviation of three separate measurements, was never larger than 2%.

3. Results and discussion

The morphology of the three ACs was analyzed by SEM (Fig. 1). The porous texture is clearly observed, showing a porous structure formed by a network of wide macropores. Some cracks also

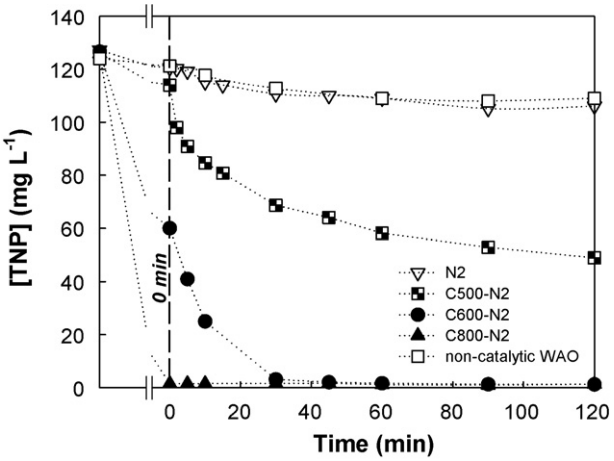

Fig. 2. Evolution of trinitrophenol concentration at 473 K and total pressure of 5.5 MPa in the absence of any carbon material and using pure nitrogen (N_2), in the presence of the ACs and using the same nitrogen atmosphere (C500-N_2, C600-N_2 and C800-N_2), and in the non-catalytic experiment using pure air instead of nitrogen (non-catalytic WAO).

appeared due to the thermal shocks and the strains generated during the process of activation of the ligno-cellulosic raw material.

The textural properties of the fresh ACs are gathered in Table 2. Increasing the activation temperature led to the development of microporosity (W_0), and consequently higher BET surface areas. Thus, the lower surface area was obtained for C500 (121 m^2 g^{-1}) and the highest for C800 (1530 m^2 g^{-1}). The increase of the activation temperature not only produces a larger development of microporosity but also a definite increase of the mean micropore width (L_0), as observed mainly for C800. There is also an increase in the meso and macropore volume (Table 2) resulting from the increase in activation temperature. Thus C800 has the highest S_{BET} and pore volumes.

The surface chemistry of the samples was characterized by TPD and pH_{PZC}, the results being summarized in Table 2. All ACs showed similar surface chemistry, as reflected on the pH_{PZC} and oxygen content. The values of pH_{PZC} are close to neutral, but slowly tend to increase. The oxygen contents show the opposite behaviour, due to the higher activation temperature used, which favours the evolution of the oxygenated surface groups from the carbon surface [30].

Fig. 2 shows the evolution of TNP concentration as a function of time in experiments performed at 473 K and total pressure of 5.5 MPa: (i) in the absence of any carbon material and using pure N_2 (blank experiment), (ii) in the presence of the ACs (C500-N_2, C600-N_2 and C800-N_2) and using the same nitrogen atmosphere (TNP adsorption processes), and (iii) in the homogeneous TNP oxidation using pure air instead of nitrogen (non-catalytic WAO). The pre-heating step is represented before 0 min in order to obtain a better picture of the complete concentration evolution from the instant that TNP is loaded into the reactor until the end of the experiment.

The results obtained without a carbon material under inert atmosphere (N_2) indicate that TNP is thermally stable at the temperature used (473 K) and that only a small fraction of TNP (ca. 10–15%) seems to be transferred to the gas phase at the conditions employed (less than 5% during the pre-heating period). Since the results obtained with air instead of nitrogen are similar in the absence of ACs, the homogeneous WAO of TNP can be neglected. As expected, the DOC after 120 min in these experiments is nearly the same as the DOC of the initial solution (about 39 mgC L^{-1}). When using the ACs under nitrogen atmosphere, a marked decrease of the TNP concentration is observed. Due to the absence of oxidant, it is evident that TNP is strongly removed by adsorption. The adsorption

Table 2
Textural and chemical properties of synthesized ACs.

Carbon	S_{BET} ($m^2\ g^{-1}$)	W_0[a] (CO_2) ($cm^3\ g^{-1}$)	L_0[b] (CO_2) (nm)	S_{ext}[c] ($m^2\ g^{-1}$)	V_{meso}[c] ($cm^3\ g^{-1}$)	V_{macro}[c] ($cm^3\ g^{-1}$)	O_{TPD} (%)	pH_{PZC}
C500	121	0.18	0.5	45	0.14	0.74	5.3	6.6
C600	423	0.22	0.6	63	0.15	0.63	5.0	6.9
C800	1530	0.45	0.7	82	0.21	0.88	3.7	7.5

[a] Resulting from the Dubinin–Radushkevich equation applied to the data obtained by adsorption of CO_2.
[b] Using the Stoeckli equation.
[c] Obtained by Hg porosimetry.

is high even during the pre-heating period, where the TNP concentration decreases by 10, 53 and 99% for C500, C600 and C800, respectively. After 120 min these values are 61% for C500 and 99% for C600 and C800. Nevertheless, in spite of C600 and C800 being able to completely remove the TNP, the adsorption process is faster on C800, which is due to its higher surface area (S_{BET} = 1530 m^2/g) and larger macro and mesopore volumes. As expected, adsorption is the lowest for C500. During the pre-heating period (before t = 0 min, conducted with 0.5 MPa of nitrogen) the amount adsorbed is very low, but increases when the nitrogen pressure is increased up to a total pressure of 5.5 MPa (after t = 0 min), denoting some diffusion problems at the lower pressure of 0.5 MPa. Therefore, it seems that accessibility problems of the solution to the narrowest microporosity, and consequently of the dissolved TNP, are present and the increase of the total pressure favours the accessibility of TNP to this range of porosity.

These results are in accordance with the enthalpy of adsorption measured for TNP (obtained at atmospheric pressure) and plotted *versus* the surface area in Fig. 3, i.e. the enthalpy of adsorption increases with the surface area, and the respective TNP removal in Fig. 2 is higher when using carbons with higher surface areas. The pH_{PZC} of the ACs range from 6.6 to 7.5 (Table 2) and the ionization constant of TNP is 4.2×10^{-1}, corresponding to a pK_a of 0.38 [36]. At the employed conditions (natural solution pH of 3.1 at the given TNP concentration) the surface of carbon materials is positively charged and the attractive electrostatic interactions favour the affinity of the carbon surface for the TNP anions. This fact has been discussed previously with other substituted phenols [37].

Fig. 4a shows the results obtained in the presence of ACs and pure air. For comparative purposes, the results of TNP adsorption on the C500 material obtained in N_2 atmosphere are also presented. When oxygen is used, the total TNP elimination is observed at 60 min while DOC removals were always higher than 80% after 120 min. Differences between both parameters indicate the formation of organic intermediates that remain in solution.

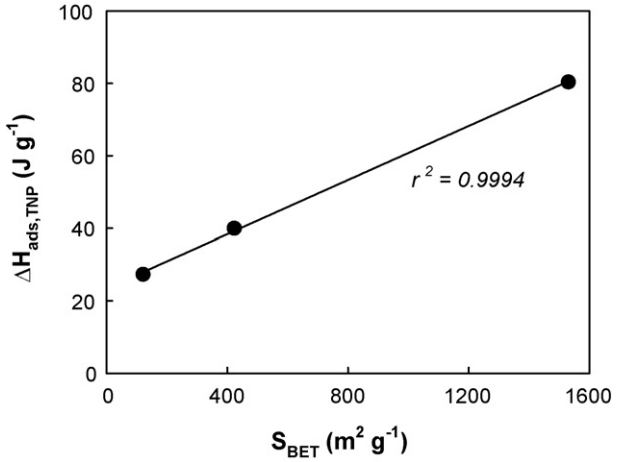

Fig. 3. Enthalpy of adsorption measured for TNP *versus* the surface area of ACs.

In order to assess the carbon activities for the oxidation of TNP in a more quantitative way, the amounts of nitrates and nitrites formed during the reaction were monitored, since they are the expected final products of TNP mineralization [6,16]. Nitrates were not observed when the experiment was conducted with pure nitrogen, or in non-catalytic oxidation (WAO), reinforcing that in these cases the small reductions in TNP concentration are due to the TNP liquid–vapour equilibrium. Similarly, neither nitrates nor nitrites were observed for C500-N_2 experiments, reinforcing that reductions in TNP concentration are due to adsorption processes without TNP decomposition. In contrast, nitrates were formed in the presence of air, independently of the properties of the carbon material used (C500-Air, C600-Air and C800-Air in Fig. 4b).

On the other hand, because the amount of nitrates in the solution (Fig. 4b) was lower than the theoretical amount expected for total mineralization, it is necessary to confirm that these results are not affected by the eventual adsorption of nitrates on these carbons. Thus, an experiment was performed with the carbon presenting

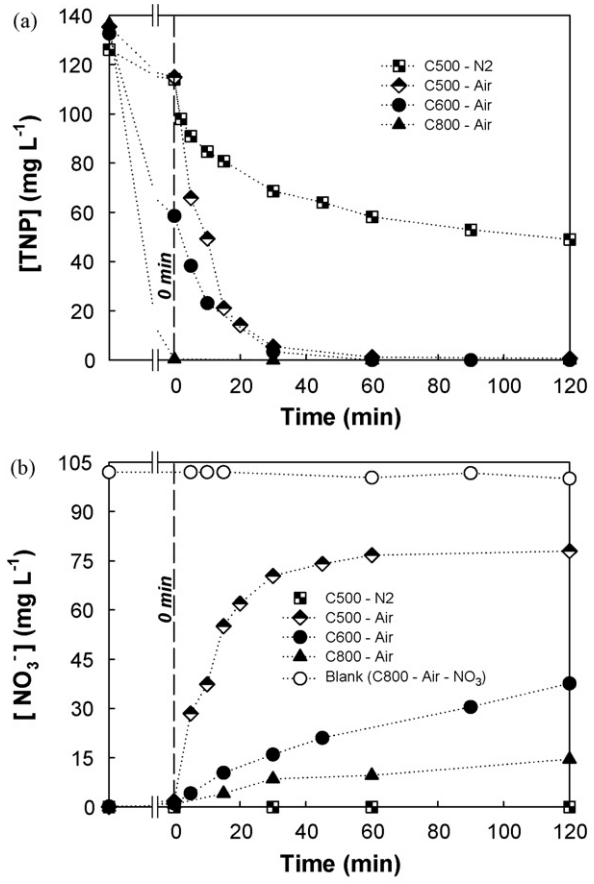

Fig. 4. Evolution of trinitrophenol concentration (a) and respective formation of nitrates (b) in CWAO at 473 K, 5.5 MPa of total pressure and 0.7 MPa of oxygen partial pressure (C500-Air, C600-Air and C800-Air) and comparison with a blank experiment (C800-Air-NO_3) performed with C800 and water containing nitrates.

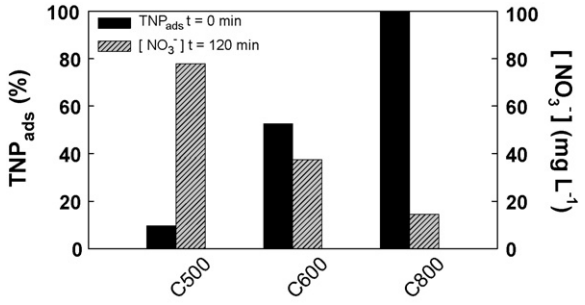

Fig. 5. Percentage of TNP adsorbed on the different ACs for $t = 0$ min together with the concentration of nitrates measured after 120 min of oxidation.

higher surface area (C800) and with water (without TNP) containing the maximum amount of nitrates that is expected based on the total mineralization of the TNP solution, referred to blank (C800-Air-NO_3) in Fig. 4b. Sodium nitrate was used as precursor of nitrates. Nitrates were not adsorbed on the activated carbon, the concentration being quite stable along the experiment. The strong correlation between the profiles obtained for TNP degradation (Fig. 4a) and formation of nitrates (Fig. 4b) indicates that nitrates can be used to follow the oxidation of TNP.

The amounts of nitrates generated in the liquid by effect of the different ACs increase with the decrease of their surface area. Nitrites were always negligible, due to the oxidizing conditions of CWAO. The amount of nitrates found in solution with C500 corresponds to around 77% of the nitrates that should be formed considering total mineralization of the TNP solution (101 mgNO_3 L^{-1}); values of 37 and 15% were found for C600 and C800, respectively. Therefore, the fast catalytic oxidation of TNP is observed with ACs presenting low S_{BET} (C500), while the TNP oxidation is less evident with the ACs that have high S_{BET} (C600 and C800). The final TNP concentration with C500 in the absence of O_2 is around 40% of the initial TNP concentration, indicating that 60% of TNP is eliminated from the solution by adsorption. However, in the presence of oxygen, the TNP degradation is at least 77%, according with the nitrate percentages. This means that both processes, adsorption and oxidation, occur simultaneously. In the case of C800, TNP adsorption is so fast that TNP was totally removed before pressurizing with air. Nevertheless, after this, the amount of nitrates in solution progressively increased with reaction time. This indicates that the TNP oxidation reaction takes place by a pure heterogeneous process.

Fig. 5 shows the percentage of TNP adsorbed on the different ACs for $t = 0$ min, together with the concentration of nitrates measured after 120 min of oxidation. With the C800 carbon the entire amount of TNP loaded into the reactor was readily adsorbed at $t = 0$; however, the adsorption capacity progressively decreases with the microporosity (surface area) of ACs obtained at progressively lower activation temperature. This is the typical behaviour of porous adsorbents. The total mineralization degree of TNP assessed by the nitrate concentration at 120 min (where the total elimination of TNP was reached independently of the carbon material used) showed an additional tendency.

With C800, it can be clearly proposed that the reaction takes place via a purely heterogeneous route, since TNP is totally adsorbed at $t = 0$ and there is a fraction of nitrates formed after 120 min. The surface of C500, although of smaller area than that of C800, presents the same initial chemical characteristics. Thus, adsorption of both TNP and O_2 can also occur in C500, and the heterogeneous catalytic process can be also developed on the C500 surface. The question is to clarify how the reaction develops in each case, taking into account the fact that the catalyst with smaller surface area promotes the reaction to a larger extent, which may seem contradictory.

Examination of fresh and used catalysts allows the identification of possible changes on the catalysts during reaction and possible interpretation of mechanisms occurring on the ACs surface. Fig. 6 shows the TPD spectra of fresh and used ACs C500 (Fig. 6a–d) and C800 (Fig. 6e–h). The total amounts of the various surface groups can be determined from the TPD spectra, since these groups are decomposed into CO (Fig. 6a, b, e and f) or/and CO_2 (Fig. 6c, d, g and h) upon heating [32,33]. For CO, the contributions are usually assigned to carboxylic anhydrides/800–900 K, phenols or hidroquinones/940–990 K, carbonyls or quinones/1090–1150 K, and a small contribution (shoulder at low temperature) attributed to acidic carboxylic groups [31,32]. Regarding CO_2, the groups are divided in strongly acidic carboxylic groups/510–600 K, weakly acidic carboxylic groups/650–750 K, carboxylic anhydrides/800–900 K and lactones/950–1050 K. Therefore, the amounts of the different surface groups were determined by deconvolution of the TPD spectra using multiple Gaussian functions based on Levenberg–Marquardt algorithm. In particular, the sharp peak observed in the CO TPD spectra of fresh and used C500 near 1050 K (Fig. 6a and b) is usually found for ACs prepared by chemical methods or for carbon materials containing traces of metals. In addition, at higher temperatures (>1200 K) the CO spectra do not return to the baseline. These situations were considered for deconvolution purposes, but they make difficult a quantitative analysis of peaks appearing at near temperatures. It can be observed in both CO and CO_2 TPD spectra of C500 and C800 that the fresh ACs have a poor concentration of oxygenated surface groups, the amounts of CO and CO_2 released from the carbon surface increasing upon use in CWAO. As can be seen, the major oxygen functional groups created on the ACs surface are phenols (–OH), carboxylic acids (–COOH) and carbonyls/quinones (=O).

The changes in the TPD spectra can be attributed to the decomposition of oxygenated organic compounds adsorbed on the surface and/or to oxygenated surface groups generated by oxidation of the carbon surface by air at the CWAO conditions. Taking into account that around 80% of TNP is totally degraded over the C500 sample, the second option seems to be more favourable. In order to confirm this hypothesis, different experiments were carried out. TPD spectra were recorded after an additional experiment performed at 473 K with the C500 material and pure water (without TNP) in the presence of air (5.5 MPa), the used sample referred as C500–H_2O. The CO and CO_2 TPD spectra obtained for the used C500 in the absence of TNP are very similar to those obtained for the used C500 in the presence of TNP (Fig. 6b and d, respectively). Therefore, the strong surface modification that occurs in C500 is attributed to the conditions employed in CWAO, and not specifically to the presence of adsorbed organic compounds (TNP or intermediates). Also, another experiment was conducted with pure water and using C800, but replacing air by pure nitrogen. Since the amount of oxygen functionalities on the carbon surface did not increase in the presence of pure nitrogen, it can be concluded that air used in CWAO plays an important role in the modification of the carbon surface chemistry. These results are also in agreement with our previous experience [16,38].

The N_2 adsorption isotherms of the samples used in catalytic and adsorption experiments are shown in Fig. 7 and the results from the textural characterization are gathered in Table 3. N_2 adsorption isotherms of type I were observed for all the fresh and used ACs, which are typical of microporous materials [39,40]. In comparison with fresh samples, an important decrease of the porosity was observed for all the samples used in CWAO, denoting that TNP (or intermediate compounds formed during TNP degradation) remains inside the micropores either after adsorption (C500-N_2 and C800-N_2) or after the catalytic process (C500-Air and C800-Air). Nevertheless, activation temperature has a clear effect on the behaviour of the different ACs.

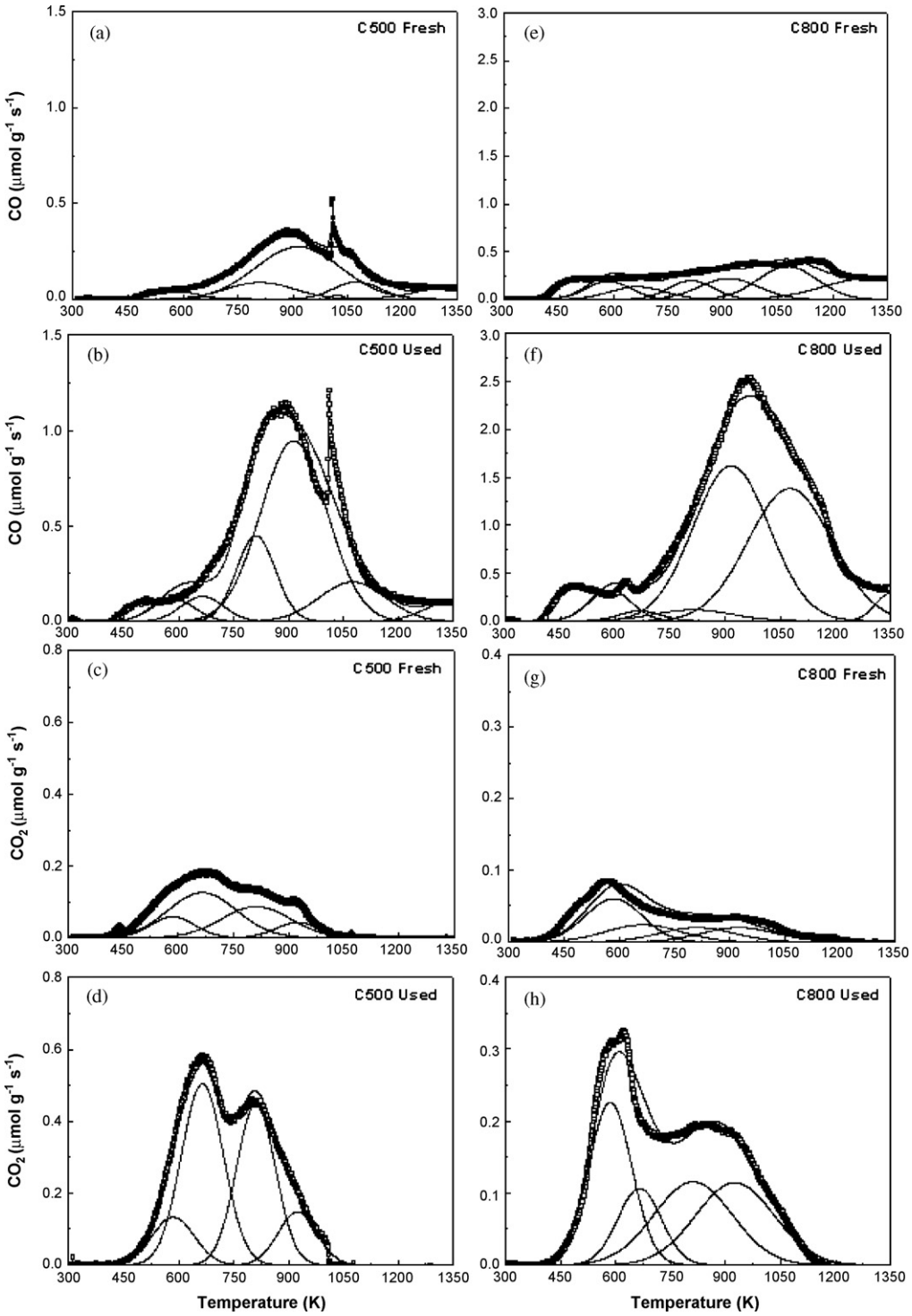

Fig. 6. TPD spectra for the fresh and used ACs catalysts C500 (a–d) and C800 (e–h) in terms of CO (a, b, e and f) and CO_2 (c, d, g and h) evolutions.

Practically total blockage of S_{BET} was observed with sample C500, prepared with the lowest activation temperature and consequently with lower micropore volume and narrower micropores (92 or 72% in N_2 or air atmosphere, respectively), while the micropore volume and S_{CO_2}, corresponding to the narrow microporosity given in Table 3, decreased only about 20% after the adsorption (C500-N_2) or the catalytic (C500-Air) process. This means that TNP adsorption occurs in a specific range of microporosity, preferably in micropores wider than 0.5 nm. In addition, the C500 sample used with pure water (without TNP) in the presence of air (C500-H_2O), presented a S_{BET} = 108 $m^2\ g^{-1}$, which is slightly lower than that of C500-Fresh (results not shown in the table). This S_{BET} decrease is explained by the oxygenated surface groups created on the carbon surface, which leads to a certain porosity blockage and to additional restrictions for the access of nitrogen molecules to the narrow micropores at 77 K.

An increase of the activation temperature leads to a larger micropore volume and wider micropores (C600 and C800). For this reason, the percentage of reduction of S_{BET} for the samples used in adsorption experiments with N_2 atmosphere is the following:

Table 3
Textural characterization of fresh and used ACs, in adsorption (-N_2) or reaction (-Air) experiments.

Carbon	S_{BET} ($m^2\,g^{-1}$)	S_{CO_2} ($m^2\,g^{-1}$)[a]	W_0[b] (CO_2) ($cm^3\,g^{-1}$)	L_0[a] (CO_2) (nm)
C500-Fresh	121	745	0.18	0.5
C500-N_2	9 (92*)	573 (23*)	0.14	0.5
C500-Air	34 (73*)	583 (22*)	0.16	0.5
C600-Fresh	423	797	0.22	0.6
C600-N_2	254 (40*)	628 (21*)	0.16	0.5
C600-Air	73 (83*)	419 (47*)	0.11	0.5
C800-Fresh	1530	1283	0.45	0.7
C800-N_2	1062 (31*)	980 (24*)	0.38	0.8
C800-Air	163 (89*)	435 (66*)	0.14	0.6

[a] Using the Stoeckli equations.
[b] Resulting from the Dubinin–Radushkevich equation applied to the data obtained by adsorption of CO_2.
* Data in parenthesis represent the percentage of S_{BET} or S_{CO_2} decrease using the respective fresh samples as reference.

92% (C500) > 40% (C600) > 31% (C800), and, therefore, an increase of the micropore diameter and volume avoids complete S_{BET} blockage during the TNP adsorption process. However, under reaction conditions (air atmosphere), the tendency observed is the opposite to that observed in N_2 atmosphere: 73% (C500) < 83% (C600) < 89% (C800), i.e. S_{BET} blockage increases with the activation temperature in CWAO, because intermediate compounds smaller than TNP can be generated during the reaction and adsorbed in the narrow micropores that are not accessible to TNP.

Regarding the narrow microporosity (S_{CO_2}), the percentage of reduction of S_{CO_2} is practically the same for all the ACs tested in N_2 atmosphere, namely 23% (C500) ≈ 21% (C600) ≈ 24% (C800), while the reduction of S_{CO_2} for the samples used in air atmosphere increased progressively as follows: 22% (C500) < 47% (C600) < 66% (C800). Therefore, the used samples C500-Air and C500-N_2 present similar S_{CO_2} values, but this behaviour is not observed with the other two ACs (C600 and C800), where the % of S_{CO_2} reduced is higher in air than in N_2 atmosphere.

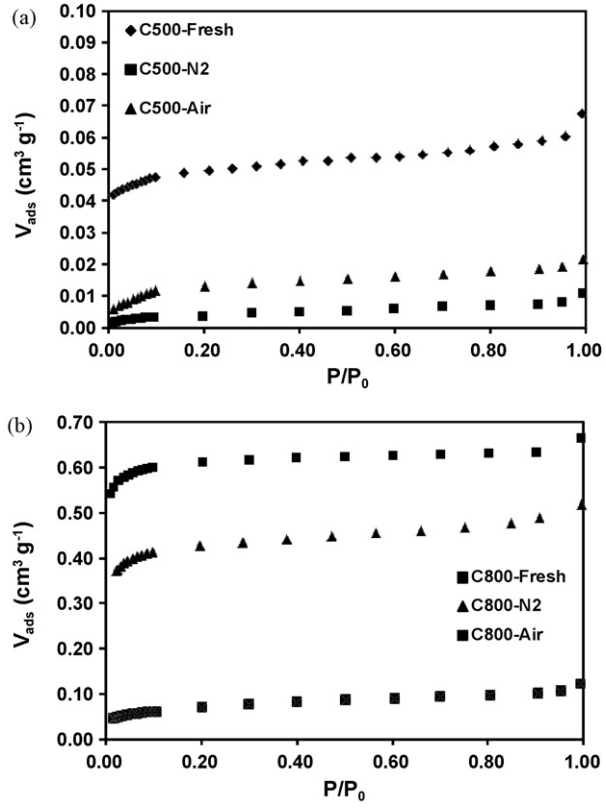

Fig. 7. N_2 adsorption isotherms at 77 K of fresh and used C500 (a) and C800 (b) materials in adsorption (-N_2) or reaction (-Air) experiments.

The textural transformation described is in agreement with the mechanism proposed. In the case of C500, the porosity is poorly developed and is the narrowest in comparison with the other ACs. Therefore it becomes quickly blocked. Thereafter, the reaction occurs on the external surface area. The adsorption of TNP in this sample must be irreversible preventing further degradation of adsorbed TNP, in such a way that C500 used in air or nitrogen atmospheres (C500-Air and C500-N_2, respectively) showed similar S_{CO_2} values. Both micropore volume and diameter increase with increasing activation temperature, which favours TNP adsorption; however, the percentage of reduction of S_{CO_2} is similar for all the ACs in N_2 atmosphere, indicating a parallel evolution of both parameters. The different textural transformations occurring in inert and oxidative conditions suggest that the oxidation of the TNP adsorbed in the micropores takes place. This is favoured because the microporosity in C800 is wider than in the case of C500. The degradation of TNP generates smaller organic compounds which can be retained into the narrow micropores, and consequently produces a larger decrease of S_{CO_2} and S_{BET}. The NO_3^- species generated during these oxidative reactions are not adsorbed by the ACs, as was also showed by the corresponding blank experiments, and are desorbed to the solution, being therefore a clear proof of the development of heterogeneous reactions inside the pores.

Thus, the high microporosity of C800 favours a quick adsorption, and the heterogeneous catalytic process is slower because the reaction must take place in the microporosity. Smaller organic compounds which can be retained into the narrow micropores and diffusion restrictions, may limit the access of the reactant (O_2) and the exit of the reaction products ($CO_2 + H_2O + NO_3^-$). In the case of C500, TNP and oxygen can be adsorbed on different surface sites, as shown by the textural and chemical characterization. Moreover, due to the lower porosity, there is a large part of TNP remaining in solution. Therefore, the reaction can take place quickly on macro–mesopores (external porous surface area) by effect of concentration of reactant, this external porous surface being quickly occupied again by additional TNP and O_2 molecules from the solution, because this porosity range does not present diffusion restrictions. This can justify the fast appearance of NO_3^- in solution. Additional experiments were performed with different mass ratios of TNP to AC. A significant higher amount of AC or a lower concentration of TNP lead to the absence of TNP in the liquid phase at $t = 0$ min, because complete adsorption of TNP occurs at low TNP to AC mass ratios. A half-load of AC ($0.1\,g\,L^{-1}$) strongly decreases the amount of TNP adsorbed at $t = 0$ min to 6, 20 and 62% for C500, C600 and C800, respectively. The amount of nitrates formed in these experiments was not significantly different after 120 min, but some variations were detected, namely 50.6, 55.9 and 59.0 $mg\,L^{-1}$ for C500, C600 and C800, respectively. These results indicate that when the ACs are all saturated at $t = 0$ min and there is a significant fraction of TNP in the liquid phase, the overall activity

of the ACs in the degradation of TNP increases with the external surface area.

4. Conclusions

The activation of biomass residues is an excellent alternative to produce suitable materials to be used for water purification. Treatments at low temperatures produce carbon materials with poorly developed microporosity that present an excellent behaviour as catalysts in CWAO process. The microporosity is progressively developed by increasing the activation temperature, and highly porous carbon materials are obtained. Two clear different situations were observed: with highly microporous carbons the liquid phase is free of TNP because a large amount of TNP is adsorbed in the micropores and little oxidation occurs in meso- and macropores (external surface area), while with poorly microporous carbons the pores are readily saturated, and there is a large amount of TNP in the bulk of liquid that can easily access to meso- and macropores, where TNP is degraded faster than in wide micropores. Some changes of the textural and chemical properties of the ACs are produced during the reaction, such as partial blockage of the microporosity and an increase of the oxygenated surface groups.

Acknowledgements

Support for this work was provided by LSRE/LCM LA financing from "Programa de Financiamento Plurianual de Unidades de I&D/Laboratórios Associados" by Fundação para a Ciência e a Tecnologia (FCT), and from the MEC-FEDER (CTQ2007-61324) for which the authors are thankful. A.M.T.S. acknowledges the financial support from POCI/N010/2006. S.M.T. and A.F.P.C. acknowledge the Spanish Ministry of Education and Science for a F.P.U. research fellowship and a Ramón y Cajal research contract, respectively.

References

[1] C. Aguilar, R. García, G. Soto-Garrido, R. Arriagada, Applied Catalysis B: Environmental 46 (2003) 229–237.
[2] F. Stüber, J. Font, A. Fortuny, C. Bengoa, A. Eftaxias, A. Fabregat, Topics in Catalysis 33 (2005) 3–50.
[3] A. Eftaxias, J. Font, A. Fortuny, A. Fabregat, F. Stüber, Applied Catalysis B: Environmental 67 (2006) 12–23.
[4] M. Santiago, F. Stüber, A. Fortuny, A. Fabregat, J. Font, Carbon 43 (2005) 2134–2145.
[5] J.P.S. Sousa, A.M.T. Silva, M.F.R. Pereira, J.L. Figueiredo, Separation Science & Technology 45 (2010) 1546–1554.
[6] V. Kavitha, K. Palanivelu, Journal of Photochemistry and Photobiology A: Chemistry 170 (2005) 83–95.
[7] J. Levec, A. Pintar, Catalysis Today 124 (2007) 172–184.
[8] M.E. Suárez-Ojeda, J. Carrera, I.S. Metcalfe, J. Font, Chemical Engineering Journal 144 (2008) 205–212.
[9] A.M.T. Silva, Materials and Technology 43 (2009) 9.
[10] S.K. Bhargava, J. Tardio, J. Prasad, K. Foger, D.B. Akolekar, S.C. Grocott, Industrial & Engineering Chemistry Research 45 (2006) 1221–1258.
[11] L. Oliviero, H. Wahyu, J. Barbier Jr., D. Duprez, J.W. Ponton, I.S. Metcalfe, D. Mantzavinos, Chemical Engineering Research and Design 81 (2003) 384–392.
[12] D. Mantzavinos, R. Hellenbrand, A.G. Livingston, I.S. Metcalfe, Applied Catalysis B: Environmental 7 (1996) 379–396.
[13] L. Oliviero, J. Barbier, D. Duprez, H. Wahyu, J.W. Ponton, I.S. Metcalfe, D. Mantzavinos, Applied Catalysis B: Environmental 35 (2001) 1–12.
[14] A. Quintanilla, N. Menéndez, J. Tornero, J.A. Casas, J.J. Rodríguez, Applied Catalysis B: Environmental 81 (2008) 105–114.
[15] A. Quintanilla, J.A. Casas, J.J. Rodríguez, Applied Catalysis B: Environmental 76 (2007) 135–145.
[16] Â.C. Apolinário, A.M.T. Silva, B.F. Machado, H.T. Gomes, P.P. Araújo, J.L. Figueiredo, J.L. Faria, Applied Catalysis B: Environmental 84 (2008) 75–86.
[17] M.E. Suarez-Ojeda, F. Stüber, A. Fortuny, A. Fabregat, J. Carrera, J. Font, Applied Catalysis B: Environmental 58 (2005) 105–114.
[18] H.T. Gomes, B.F. Machado, A. Ribeiro, I. Moreira, M. Rosário, A.M.T. Silva, J.L. Figueiredo, J.L. Faria, Journal of Hazardous Materials 159 (2008) 420–426.
[19] T. Cordero, J. Rodríguez-Mirasol, J. Bedia, S. Gomis, P. Yustos, F. García-Ochoa, A. Santos, Applied Catalysis B: Environmental 81 (2008) 122–131.
[20] A. Quintanilla, J.A. Casas, J.J. Rodriguez, Applied Catalysis B: Environmental 93 (2010) 339–345.
[21] J.L. Figueiredo, M.F.R. Pereira, Catalysis Today 150 (2010) 2–7.
[22] S. Yang, W. Zhu, X. Li, J. Wang, Y. Zhou, Catalysis Communications 8 (2007) 2059–2063.
[23] S. Yang, X. Li, W. Zhu, J. Wang, C. Descorme, Carbon 46 (2008) 445–452.
[24] F. Rodríguez-reinoso, Carbon 36 (1998) 159–175.
[25] R. Ubago-Pérez, F. Carrasco-Marín, D. Fairén-Jiménez, C. Moreno-Castilla, Microporous and Mesoporous Materials 92 (2006) 64–70.
[26] S. Brunauer, P.H. Emmett, E. Teller, Journal of the American Chemical Society 60 (1938) 309–319.
[27] D. Fairén-Jiménez, F. Carrasco-Marín, C. Moreno-Castilla, Carbon 44 (2006) 2301–2307.
[28] F. Stoeckli, A. Guillot, A.M. Slasli, D. Hugi-Cleary, Carbon 40 (2002) 383–388.
[29] R.C. Bansal, J.B. Donnet, F. Stoeckli (Eds.), Active Carbon, Marcel Dekker, New York, 1988.
[30] C. Moreno-Castilla, F. Carrasco-Marín, F.J. Maldonado-Hódar, J. Rivera-Utrilla, Carbon 36 (1998) 145–151.
[31] C. Moreno-Castilla, F. Carrasco-Marín, A. Mueden, Carbon 35 (1997) 1619–1626.
[32] J.L. Figueiredo, M.F.R. Pereira, M.M.A. Freitas, J.J.M. Órfão, Carbon 37 (1999) 1379–1389.
[33] J.L. Figueiredo, M.F.R. Pereira, M.M.A. Freitas, J.J.M. Órfão, Industrial & Engineering Chemistry Research 46 (2007) 4110–4115.
[34] C. Moreno-Castilla, F. Carrasco-Marín, C. Parejo-Pérez, M.V. López Ramón, Carbon 39 (2001) 869–875.
[35] F. Carrasco-Marín, D. Fairén-Jiménez, C. Moreno-Castilla, Carbon 47 (2009) 463–469.
[36] F.A. Carey (Ed.), Organic Chemistry, 2nd ed., McGRAW-HILL Inc., New York, 1992, p. 984.
[37] C. Moreno-Castilla, J. Rivera-Utrilla, M.V. López-Ramón, F. Carrasco-Marín, Carbon 33 (1995) 845–851.
[38] A.M.T. Silva, B.F. Machado, J.L. Figueiredo, J.L. Faria, Carbon 47 (2009) 1670–1679.
[39] K.S.W. Sing, Pure and Applied Chemistry 57 (1985) 603–619.
[40] H. Marsh, F. Rodríguez-Reinoso, Activated Carbon Elsevier (2006).